



# Conservation of dissolved organic matter molecular composition during mixing of the deep water masses of the northeast Atlantic Ocean



Roberta L. Hansman<sup>a,\*</sup>, Thorsten Dittmar<sup>b,c</sup>, Gerhard J. Herndl<sup>a,d</sup>

<sup>a</sup> Department of Limnology and Oceanography, University of Vienna, Vienna, Austria

<sup>b</sup> Research Group for Marine Geochemistry (ICBM-MPI Bridging Group), Institute for Chemistry and Biology of the Marine Environment (ICBM), Carl von Ossietzky University of Oldenburg, Oldenburg, Germany

<sup>c</sup> Max Planck Institute for Marine Microbiology (MPI), Bremen, Germany

<sup>d</sup> Department of Biological Oceanography, Royal Netherlands Institute for Sea Research (NIOZ), Den Burg, The Netherlands

## ARTICLE INFO

### Article history:

Received 20 January 2015

Received in revised form 21 May 2015

Accepted 1 June 2015

Available online 4 June 2015

### Keywords:

Marine dissolved organic matter

FT-ICR-MS

North Atlantic

Carbon cycle

## ABSTRACT

Characterizing the composition of marine dissolved organic matter (DOM) is important for gaining insight into its role in oceanic biogeochemical cycles. Using Fourier transform ion cyclotron resonance mass spectrometry, we analyzed the molecular composition of solid phase extracted (SPE) DOM from the northeast Atlantic to investigate the specificity of the DOM pool of the individual major water masses of the North Atlantic. All 272 measured samples from depths ranging from 87 to 5609 m and latitudes from 24°N to 68°N shared 96% similarity (on a Bray–Curtis scale) in their DOM composition. Small variations between subsurface and deep samples and among latitudinal groupings were identified, but overall, water mass specific SPE-DOM composition was not apparent. A strong correlation between a calculated degradation index and water mass age indicates variability in portions of the DOM pool, and ocean-scale differences were observed between the North Atlantic and deep North Pacific. However, within the deep northeast Atlantic, conservative mixing primarily drives the molecular composition of SPE-DOM.

© 2015 The Authors. Published by Elsevier B.V. This is an open access article under the CC BY-NC-ND license (<http://creativecommons.org/licenses/by-nc-nd/4.0/>).

## 1. Introduction

With an inventory of 662 Pg C, marine dissolved organic matter (DOM) is one of the largest active pools of carbon on the planet and is comparable in size to atmospheric CO<sub>2</sub> (Hansell et al., 2009; Hedges, 1992). Produced mainly by primary production in surface waters (Carlson, 2002), DOM serves as the dominant substrate for heterotrophic microbes throughout the water column (Azam et al., 1983). Marine DOM can be described by its reactivity and age along a continuum ranging from labile to refractory and on timescales of hours to thousands of years (Follett et al., 2014; Hansell et al., 2012; Kirchman et al., 1991). Though the majority of the marine DOM pool is thought to be recalcitrant, gradients in reactivity exist vertically throughout the water column and laterally in the open ocean (Hansell, 2013; Hansell et al., 2012). Abiotic processes such as photo-degradation in surface waters contribute to these gradients, as well as both the production and remineralization of marine DOM by microbial communities throughout the water column.

Characterizing marine DOM has been a challenge for many years, primarily due to its complexity and low concentration relative to the inorganic salts present in seawater. The composition of parts of the DOM

pool has been discerned by quantifying specific biochemical groups (e.g., amino acids, carbohydrates) and/or size classes using several techniques such as ultrafiltration, NMR, and HPLC (Aluwihare et al., 1997; Benner, 2002; Benner et al., 1992; McCarthy et al., 1998; Pakulski and Benner, 1994), but the molecular structure of the majority of marine DOM remains elusive. Recently, ultrahigh resolution Fourier transform ion cyclotron resonance mass spectrometry (FT-ICR-MS) has been used with electrospray ionization (ESI) to characterize marine DOM at a molecular level (Chen et al., 2014; Dittmar and Paeng, 2009; Flerus et al., 2012; Hertkorn et al., 2006; Koch et al., 2005; Kujawinski et al., 2009; Medeiros et al., 2015). Mass accuracies within 1 ppm allow for the assignment of elemental formulas to thousands of peaks resolved from marine DOM, establishing a molecular fingerprint for each particular seawater sample. Though still subject to the limitations of the method used to isolate marine DOM, FT-ICR-MS provides another useful tool available for further characterizing the composition of the oceanic DOM pool.

The North Atlantic is comprised of several well-characterized water masses with distinct physical and chemical attributes (van Aken, 2000a, b). These include cold and typically less saline Lower Deep Water (LDW) from the south, Iceland–Scotland Overflow Water (ISOW) and Labrador Sea Water (LSW) from the north, and warm salty Mediterranean Sea Outflow Water (MSOW) emanating from the Strait of Gibraltar (Table S1). The North Atlantic is also the site of North Atlantic Deep Water (NADW) formation, where cold and saline surface water

\* Corresponding author at: Department of Limnology and Oceanography, University of Vienna, Althanstrasse 14, 1090 Vienna, Austria.  
E-mail address: [rhansman@gmail.com](mailto:rhansman@gmail.com) (R.L. Hansman).

sinks into the deep ocean's interior in the Greenland–Iceland–Norwegian Sea. The formation of NADW leads to the export of DOM from the euphotic layer to meso- and bathypelagic depths where microbes remineralize a portion of this DOM as it is transported southward in the NADW. These processes lead to prominent vertical and latitudinal gradients in dissolved organic carbon (DOC), ranging from up to 80  $\mu\text{M}$  in surface waters to 40  $\mu\text{M}$  in the deep North Atlantic (Carlson et al., 2010). From a biological perspective, studies have also shown that distinct microbial communities and activities exist within the water masses and depth layers of the North Atlantic (Agogué et al., 2008, 2011; Sintès et al., 2013; Varela et al., 2008a,b). The northeast core of NADW (NEADW) is comprised primarily of four source water types: ISOW, LSW, LDW, and MSOW (Table S2).

In this study we used FT-ICR-MS to characterize solid-phase extracted (SPE) marine DOM in the northeast Atlantic, focusing primarily on the deep waters below 200 m. We hypothesized that the molecular composition of SPE-DOM would exhibit water mass specific signatures, shaped by the combination of physical, chemical, and biological attributes that are unique to each distinct depth layer. We further focused on specific components of our data, using a degradation index (Flerus et al., 2012) to evaluate aging of the DOM pool, and on a subset of samples to investigate the impact of water mass mixing on the molecular composition of DOM within the core of NEADW.

## 2. Methods

### 2.1. Sampling

Samples were collected from 46 stations spanning a transect from approximately 67°N to 24°N in the eastern basin of the North Atlantic as part of the Microbial Ecology of the Deep Atlantic (MEDEA) project (Fig. 1). The stations were sampled during two cruises on the RV *Pelagia*: MEDEA-1 (49°N to 24°N in October and November 2011) and MEDEA-2 (49°N to 67°N in June and July 2012). Seawater was collected in 25-L Niskin bottles from generally six depths per station corresponding to identified water masses determined primarily from potential temperature and salinity data (van Aken, 2000a,b) or distinct physical-chemical features in the water column (Table S1). Conductivity (salinity), temperature, pressure, and oxygen (SBE 43, Seabird) were measured using a Seabird CTD-system mounted on the rosette. Potential temperature ( $\theta$ ) and apparent oxygen utilization (AOU) were calculated using Ocean Data View 4.6.2 (Schlitzer, 2013).

### 2.2. Nutrients and dissolved oxygen

Concentrations of nitrate and silicate were measured on a continuous flow auto-analyzer (AxFlow Bran + Luebbe Traacs800) onboard following JGOFS recommended protocols (Gordon et al., 1993). Dissolved oxygen concentrations from the CTD sensor were checked and calibrated via Winkler titrations. Samples were collected for DOC concentrations, but unfortunately contamination and analysis problems resulted in unreliable data.

### 2.3. SPE-DOM and FT-ICR-MS

SPE-DOM was obtained from 5 L of unfiltered seawater after acidifying (pH 2 with 25% HCl) and loading it onto commercially available modified styrene divinyl benzene polymer cartridges (PPL, Agilent) (Dittmar et al., 2008). As the contribution of particulate material to the total organic matter pool in the open ocean has been shown to be small and essentially negligible in the deep ocean (i.e., <4% in the Sargasso Sea water column; Hansell and Carlson, 2001; Kaiser and Benner, 2009), these unfiltered samples were presumed to be predominantly organic matter in the dissolved phase (DOM). Following extraction, cartridges were rinsed with acidified ultrapure water, dried under nitrogen, and eluted with 8 mL methanol into amber glass vials that

were then stored at  $-20\text{ }^\circ\text{C}$ . Resulting SPE-DOM samples were diluted to approximately 15 ppm in 1:1 methanol:ultrapure water and run in negative ion mode on a 15 Tesla Solarix Fourier-transform ion cyclotron resonance mass spectrometer (FT-ICR-MS; Bruker Daltonics) with an electrospray ionization source (Bruker Apollo II).

SPE-DOM from large volumes of North Equatorial Pacific Intermediate Water (NEqPIW) collected at 670 m depth off Kona, Hawaii (Green et al., 2014), was used as an in-house reference sample (Osterholz et al., 2014; Riedel and Dittmar, 2014). This reference sample was analyzed by FT-ICR-MS every day that MEDEA cruise samples were analyzed, and was used to assess and correct for instrument variability over time.

### 2.4. Data analysis

The Data Analysis software package (Bruker Daltonics) was used to calibrate FT-ICR-MS spectra with an internal calibration list, and in-house Matlab routines were used to process the resulting mass-to-charge ( $m/z$ ), resolution, and intensity for each peak in all samples. A method detection limit (MDL; Riedel and Dittmar, 2014) was established and used to filter FT-ICR-MS data. Masses present in only one sample were removed as well as those with a maximum signal-to-noise ratio less than four across all samples. Peaks present in less than 20% of samples that had a maximum signal-to-noise ratio less than 20 were also removed. Data were then normalized to the sum of all peak intensities with signal-to-noise ratios greater than five in each sample. Molecular formulas were assigned following the guidelines established in Koch et al. (2007) using the elements C, H, O, N, S, and P. Molecular indices were calculated for each assigned molecular formula to assess the degree of unsaturation (double-bond equivalents, DBE) and aromaticity (aromaticity index and modified aromaticity index, AI and AI<sub>mod</sub>) (Koch and Dittmar, 2006). The formulas for these calculations are included in the Supplementary Material.

The degradation index ( $I_{\text{deg}}$ ) was calculated for each sample with the formula developed by Flerus et al. (2012) that uses the intensities of ten compounds that correlated strongly either negatively or positively with the radiocarbon age of the DOM extracts in their study. The formula and peaks used for this calculation are included in the Supplementary Material (Table S3).

Multivariate statistics including principal component analysis (PCA) and canonical analysis of principal coordinates (CAP) (Anderson and Willis, 2003) were performed using the vegan package (Oksanen et al., 2013) in R (R Core Team, 2014). Distance matrices (Euclidean for PCA, Bray–Curtis for CAP) were calculated using the normalized peak intensities described above. As a constrained ordination method, CAP was used to test for associations between SPE-DOM molecular composition and other environmental factors, including sample depth and latitude.

### 2.5. Mixing model

The contribution of four specific water types forming the NEADW sampled during the MEDEA cruises was calculated using the model presented in Reinthaler et al. (2013). Briefly, a set of linear mixing equations conserving potential temperature ( $\theta$ ), salinity ( $S$ ), and silicate concentration ( $\text{SiO}_4$ ) were solved with the additional constraint that all contributions from the four water types must total to 100%. The parameters used in the model for the MSOW (Álvarez et al., 2004), LDW, LSW, and ISOW end-members are listed in Table S2. To test whether the molecular composition of SPE-DOM is a conservative parameter in the NEADW core, the resulting contributions of each water type to the NEADW samples were then used to calculate expected FT-ICR-MS spectra for each sample collected within the NEADW using the average SPE-DOM molecular composition from 4 to 6 samples of identified end-members. This calculated data set was then compared to the actual SPE-DOM molecular compositions we measured in NEADW samples.

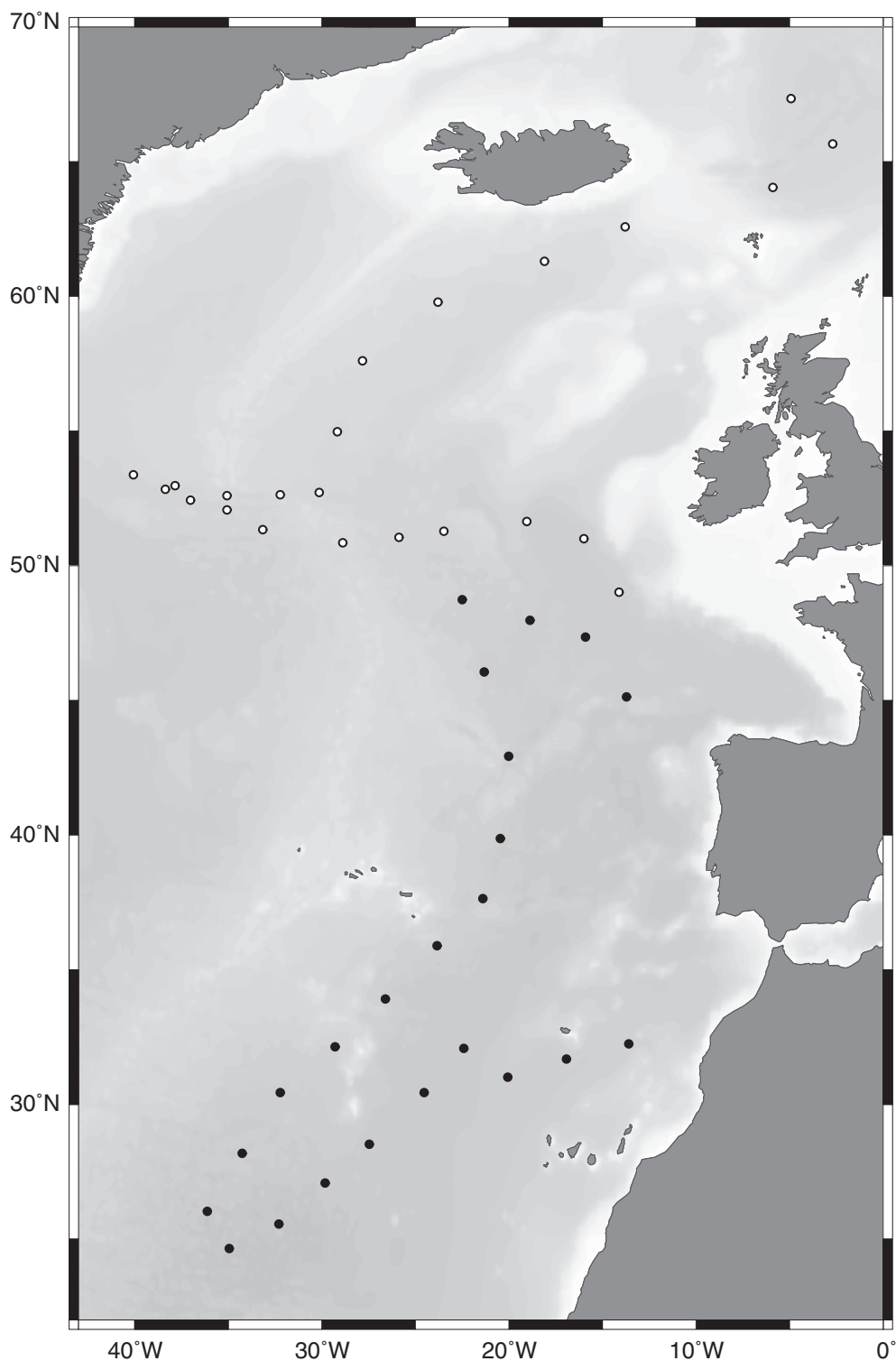


**Fig. 1.** Map of stations sampled during MEDEA cruises in fall 2011 (MEDEA-1; closed circles) and summer 2012 (MEDEA-2; open circles). Map created using Ocean Data View (Schlitzer, 2013).

### 3. Results and discussion

#### 3.1. Sampled water masses

Samples were collected throughout the deep North Atlantic (>200 m) from nine different water masses and depth layers, as

determined primarily by potential temperature and salinity data (van Aken, 2000a,b): LDW, NEADW, Antarctic Intermediate Water (AAIW), MSOW, the Oxygen Minimum ( $O_2$  min), LSW, ISOW, North Atlantic Central Water (NACW), and Norwegian Sea Deep Water (NSDW). For comparison, the Subsurface Layer (SSL; ~100 m) was also sampled at each station. Average values of selected physical–chemical

properties of the sampled water masses (salinity, potential temperature, oxygen concentration, apparent oxygen utilization (AOU), and nitrate concentration ( $\text{NO}_3$ )) are shown in Table S1.

Potential temperature ranged from  $-0.97$  °C at 3200 m in the NSDW to  $21.97$  °C in the SSL of the southernmost occupied station. The highest salinity of 37.26 was also measured for that same 100 m sample from  $24.67^\circ\text{N}$ , compared to a low of 34.71 in the SSL at  $52.73^\circ\text{N}$ , though average salinities for each sampled water mass spanned a fairly narrow range (34.91–35.76). Though the depth layer with the lowest dissolved oxygen concentration was sampled for each station ( $\text{O}_2$  min), all sampled water was well oxygenated with concentrations ranging from  $143.3$  to  $301.6$   $\mu\text{mol kg}^{-1}$ . AOU and  $\text{NO}_3$  were generally proportional to each other, increasing with depth and from north to south along the sampled transect in the deeper NEADW core. This correlation demonstrates the biological utilization of oxygen to remineralize organic material to its inorganic constituents, and serves as a proxy for the aging of subsurface water masses.

### 3.2. FT-ICR-MS of SPE-DOM

A total of 7909 masses were identified from the mass spectra in the entire MEDEA data set, with 4384 of those assigned a molecular formula; most of the non-assigned masses were  $^{13}\text{C}$  isotopologues. The average number of masses and assigned formulas for the 272 MEDEA samples are summarized in Table 1. The vast majority (99.2%) of assigned molecular formulas were shared among the general depth layers sampled during the MEDEA cruises (subsurface, mesopelagic, and bathypelagic). The elemental composition and calculated molecular indices for SPE-DOM from these layers are all also remarkably similar, with slight differences apparent between subsurface and deep samples (Table 1).

Within the MEDEA samples, variation in molecular SPE-DOM composition was low as the maximum Bray-Curtis dissimilarity for the entire North Atlantic data set, after correcting for analytical variability using the NEqPIW reference (14.7%), is only 4.0%; therefore, all samples are at least 96% similar in their composition. This similarity is remarkably high as it spans more than 5500 m of the vertical water column and  $42^\circ$  of latitude ( $67.35^\circ\text{N}$  to  $24.67^\circ\text{N}$ ). The physical and chemical properties of the water masses sampled are much more variable as gradients in temperature, salinity, and nutrient concentrations exist vertically throughout the water column and geographically with latitude. The water masses of the North Atlantic are well characterized by

these physical and chemical attributes (van Aken, 2000a,b), yet the molecular composition of SPE-DOM does not appear to be so specific. Although the first and second axes of a principal component analysis of the MEDEA data set describe 50.9% and 11.6%, respectively, of the variability in SPE-DOM molecular composition, no clear separation of samples by water mass or depth layer is evident from the PCA alone (Fig. S1).

### 3.3. Identifying variation in SPE-DOM molecular composition

Canonical analysis of principle coordinates (CAP) (Anderson and Willis, 2003) was used to evaluate associations of SPE-DOM molecular composition with sampling depth and latitude. Through this constrained ordination,  $\sim 10\%$  of the variation we observed in SPE-DOM composition throughout the North Atlantic can be described by these two parameters. Each of the canonical axes correlated with either depth or latitude (Pearson product-moment correlation coefficients  $r$  of 0.66 and 0.32, respectively;  $p < 0.001$  for both), and four distinct groups were identified by  $k$ -means clustering based on these parameters (Fig. 2).

Along the first canonical axis, there is a separation between samples collected in subsurface waters compared to those collected in the meso- and bathypelagic layers. A closer look at the differences in the average composition between these two groups of samples (Fig. 3) shows a shift to molecules with higher  $m/z$  (weighted average  $\pm$  one standard deviation:  $465 \pm 73$ ) in deep-water samples compared to those from the subsurface zone ( $336 \pm 84$ ). These differences between the subsurface and deep ocean may be due to the production of lower molecular weight compounds in surface waters and/or the accumulation of larger molecules at depth. Looking at the assigned formulas for these molecules on a van Krevelen diagram shows a shift in the average hydrogen-to-carbon (H/C) ratio from 1.39 in subsurface samples to 1.15 in deep samples, and a shift in the average oxygen-to-carbon (O/C) ratio from 0.45 to 0.51 from subsurface to deep (Fig. S2). The decrease in H/C from subsurface to deep is similar to that observed by Chen et al. (2014) for DOM isolated by reverse osmosis coupled with electrodialysis, and, as proposed by the authors, this could be due to photo-degradation of aromatic compounds in surface waters coupled with bio-degradation of aliphatic and carbohydrate-like compounds in the deeper layers.

With regard to latitude, the group of deep samples can be further divided along the second canonical axis into those samples collected from

**Table 1**

Summary of number of peaks, assigned molecular formulas (MF), elemental composition, and calculated molecular indices for FT-ICR-MS data of SPE-DOM from depth layers sampled during MEDEA cruises and replicate North Equatorial Pacific Intermediate Water (NEqPIW) reference samples. Values are peak intensity weighted averages  $\pm$  one standard deviation.

	All MEDEA	Subsurface	Mesopelagic	Bathypelagic	NEqPIW
<i>General</i>					
Number of samples	272	46	64	162	47
Depth range (m)	87–5609	87–105	249–1007	1050–5609	670
Number of peaks	$6144 \pm 422$	$6024 \pm 258$	$6202 \pm 383$	$6155 \pm 467$	$6123 \pm 286$
Number of assigned MF	$3722 \pm 213$	$3675 \pm 130$	$3755 \pm 183$	$3722 \pm 240$	$3791 \pm 97$
% of masses with assigned MF	$61 \pm 1$	$61 \pm 1$	$61 \pm 1$	$61 \pm 1$	$62 \pm 4$
Average $m/z$ of all peaks	$411 \pm 4$	$407 \pm 3$	$412 \pm 4$	$412 \pm 4$	$431 \pm 4$
<i>Elemental composition</i>					
Average C	$19.54 \pm 0.23$	$19.35 \pm 0.19$	$19.54 \pm 0.21$	$19.59 \pm 0.22$	$20.34 \pm 0.17$
Average H	$24.67 \pm 0.32$	$24.56 \pm 0.26$	$24.66 \pm 0.31$	$24.70 \pm 0.33$	$25.51 \pm 0.21$
Average O	$9.17 \pm 0.12$	$9.06 \pm 0.11$	$9.19 \pm 0.11$	$9.20 \pm 0.11$	$9.65 \pm 0.10$
Average N	$0.32 \pm 0.01$	$0.32 \pm 0.01$	$0.33 \pm 0.01$	$0.33 \pm 0.01$	$0.38 \pm 0.01$
Average P	$0.01 \pm 0.00$	$0.01 \pm 0.00$	$0.01 \pm 0.00$	$0.01 \pm 0.00$	$0.02 \pm 0.00$
Average S	$0.04 \pm 0.00$	$0.04 \pm 0.01$	$0.04 \pm 0.00$	$0.04 \pm 0.00$	$0.06 \pm 0.00$
Average O/C	$0.47 \pm 0.01$	$0.47 \pm 0.01$	$0.47 \pm 0.01$	$0.47 \pm 0.01$	$0.48 \pm 0.00$
Average H/C	$1.27 \pm 0.01$	$1.27 \pm 0.00$	$1.26 \pm 0.00$	$1.26 \pm 0.00$	$1.26 \pm 0.00$
<i>Molecular indices</i>					
Average DBE	$8.39 \pm 0.10$	$8.25 \pm 0.08$	$8.40 \pm 0.08$	$8.43 \pm 0.08$	$8.80 \pm 0.07$
Average AI	$0.18 \pm 0.00$	$0.18 \pm 0.00$	$0.18 \pm 0.00$	$0.18 \pm 0.00$	$0.19 \pm 0.00$
Average AI <sub>mod</sub>	$0.25 \pm 0.00$				

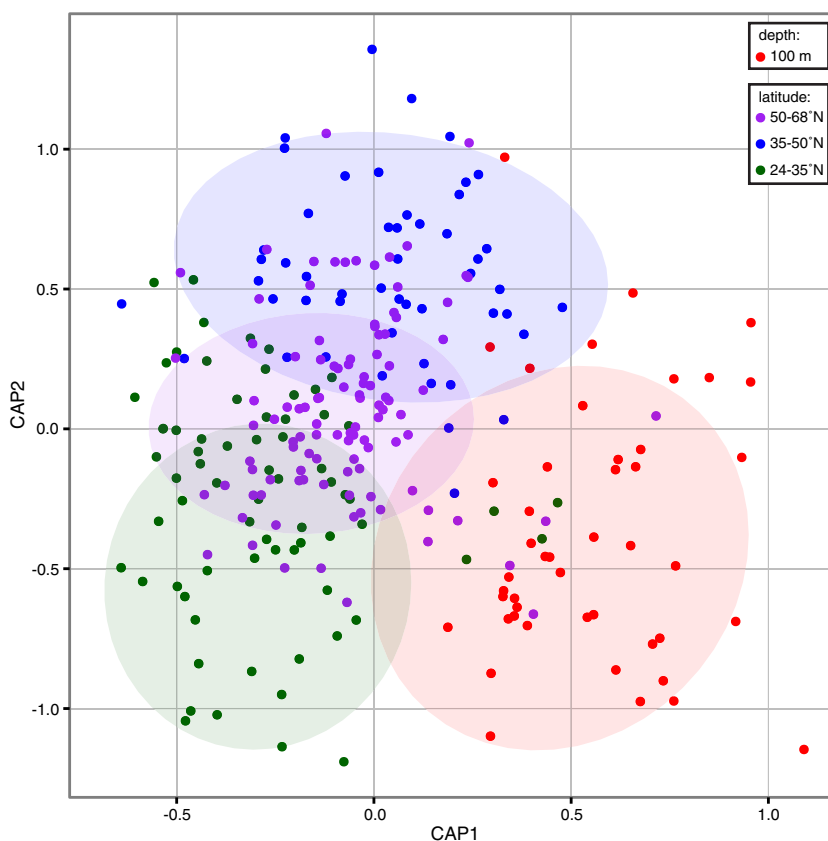


**Fig. 2.** Canonical analysis of principal coordinates of MEDEA SPE-DOM samples with sampling depth and latitude. Samples are color-coded as subsurface layer (~100 m depth) or by latitudinal group (24–35°N, 35–50°N, 50–68°N). Elliptical shading indicates 95% confidence of *k*-means clusters.

high (50–68°N), middle (35–50°N), and lower (24–35°N) latitudes (Fig. 2). The differences in the average SPE-DOM composition for each of these groups of samples are less distinct and more difficult to describe as compared to the subsurface versus deep samples (Fig. S3). However, the van Krevelen diagrams of the assigned formulas that had higher average intensities for each latitudinal group as compared to the other two groups do show shifts in primarily the O/C ratios from samples collected from high, middle, and lower latitudes within the deep North Atlantic (Fig. 4). This geographical

variation in SPE-DOM composition is perhaps not so surprising when viewed in the context of differential DOC removal rates, as presented in Hansell et al. (2012). Latitudinal variability in the removal of semi-labile, semi-refractory, and refractory components of the DOM pool could be reflected in the molecular composition of SPE-DOM throughout the North Atlantic.

#### 3.4. Degradation index

Flerus et al. (2012) proposed a degradation index ( $I_{deg}$ ) calculated from the intensities of ten FT-ICR-MS peaks that correlated with  $\Delta^{14}C$  values of SPE-DOM, providing a simple method for estimating the relative age of SPE-DOM. Although we do not have the supporting radiocarbon data for comparison, we applied this calculation to our samples and determined that the degradation indices for the entire MEDEA data set ranged from 0.649 to 0.805, with an average  $\pm$  one standard deviation of  $0.744 \pm 0.029$  (Table 2). When averaged by water mass (Table 2), there is a general trend of increasing  $I_{deg}$  with increasing depth and water mass age. This is further illustrated by the linear relationship between  $I_{deg}$  and apparent oxygen utilization (AOU) (Fig. 5). The strong correlation (Pearson product-moment correlation coefficient  $r$  of 0.79;  $p < 0.001$ ) between  $I_{deg}$  and AOU suggests the aging of components of the DOM pool as oxygen is utilized and the age of the sampled water mass increases. This is particularly notable when following the core of the NEADW southward from its area of formation in the north. Overall, however, we observed a stronger correlation between  $I_{deg}$  and AOU in the upper 1000 m of our data set as compared to samples from the bathypelagic realm (Pearson product-moment correlation coefficients  $r$  of 0.86 and 0.68, respectively;  $p < 0.001$  for both), so there is a decoupling of this relationship with depth in the northeast Atlantic. The relationship between DOC concentration and AOU in the upper

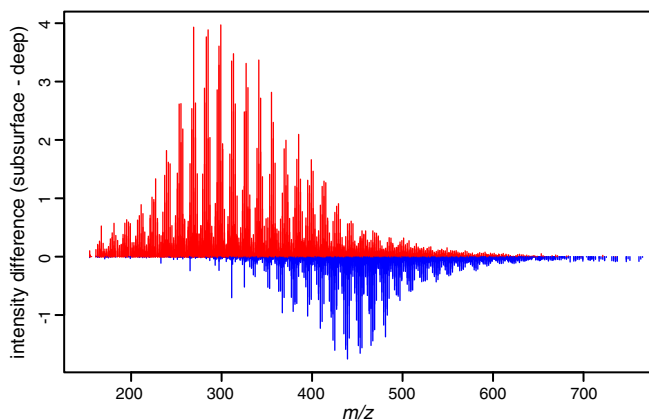


**Fig. 3.** Difference in average SPE-DOM molecular composition between subsurface layer samples and deep samples, calculated from normalized intensities and plotted against *m/z*. Peaks with higher intensities in subsurface samples are shown in red and those higher in deep samples in blue.

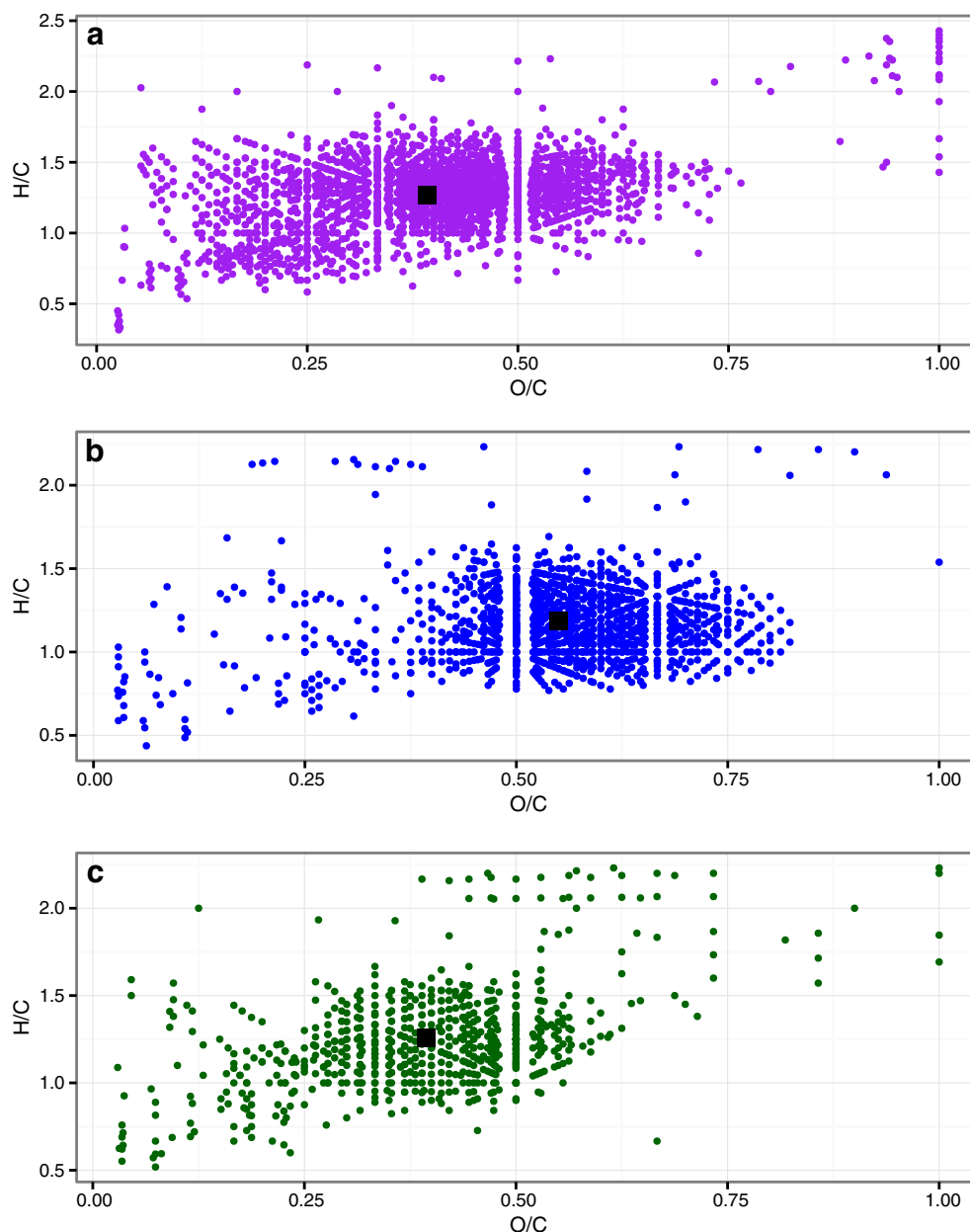


**Fig. 4.** Van Krevelen diagrams showing ratios of hydrogen-to-carbon (H/C) and oxygen-to-carbon (O/C) for assigned molecular formulas that had higher average intensities in samples collected from deep waters at high (50–68°N; a), middle (35–50°N; b), and lower (24–35°N; c) latitudes as compared to the other two groups. Average ratios for all formulas in each plot are indicated by black squares.

water column of the Atlantic subtropical gyres was used by Pan et al. (2014) to infer the remineralization of DOC, and our calculated  $I_{deg}$  implies that at least part of the contribution of DOC degradation to AOU is likely reflected in the molecular composition of SPE-DOM.

Differences in  $I_{deg}$  also highlight the fact that although the overall composite of SPE-DOM does not show significant changes throughout the North Atlantic in the principal component analysis, distinct changes in specific molecules or groups of molecules are evident. This is notable regarding future analyses of FT-ICR-MS data from marine SPE-DOM, which should focus on identifying compounds or combinations of compounds, such as the mass peaks involved in calculating  $I_{deg}$ , that can give insight into the biological, physical, and chemical processes affecting the DOM pool. An important task would be the identification of correlating or co-occurring molecules and specific groups of microbes to further our understanding of the processes through which marine microbial communities and the DOM pool are linked.

### 3.5. Comparison of MEDEA and NEqPIW SPE-DOM

The NEqPIW SPE-DOM reference sample was used primarily to assess and correct for instrument variation over time. However, it also serves as an end member for deep ocean circulation and refractory DOC (Hansell, 2013), which invites a comparison between the molecular composition of SPE-DOM from our MEDEA samples collected in the northeast Atlantic and the NEqPIW reference sample. Although the MEDEA samples and NEqPIW reference shared 98.4% of assigned molecular formulas, some differences in their individual constituents and indices were evident (Table 1). Notably, the NEqPIW reference had higher average  $m/z$ , C, H, O, N, and DBE compared to samples from the northeast Atlantic. Indeed multivariate statistics using a composite of masses and intensities with assigned molecular formulas for each sample show a clear separation between these two groups. A PCA divides the MEDEA samples and NEqPIW reference samples along the first

**Table 2**

Average ( $\pm$  one standard deviation) degradation index ( $I_{\text{deg}}$ ) of SPE-DOM as calculated from Flerus et al. (2012) for sampled MEDEA water masses and replicate NEqPIW reference samples.  $n$  = number of samples; for water mass abbreviations see Methods section and Table S1.

	$I_{\text{deg}}$	$n$	Depth range (m)
All MEDEA samples	0.744 ( $\pm$ 0.029)	272	87–5609
LDW	0.774 ( $\pm$ 0.019)	34	3000–5609
NEADW	0.760 ( $\pm$ 0.018)	41	2748–3206
AAIW	0.755 ( $\pm$ 0.016)	26	1147–1720
MSOW	0.756 ( $\pm$ 0.013)	22	619–1720
O <sub>2</sub> min	0.747 ( $\pm$ 0.016)	33	251–992
LSW	0.746 ( $\pm$ 0.011)	40	750–2233
ISOW	0.747 ( $\pm$ 0.011)	8	1050–2900
NACW	0.733 ( $\pm$ 0.010)	8	300–500
NSDW	0.737 ( $\pm$ 0.019)	14	249–3200
SSL	0.696 ( $\pm$ 0.016)	46	87–105
NEqPIW reference	0.855 ( $\pm$ 0.010)	47	670

principal component, which explains 67.6% of the variability in the data set (Fig. S4).

Differences in the average SPE-DOM composition between the MEDEA samples and the NEqPIW reference show an enrichment in lower molecular weight compounds in the water column of the northeast Atlantic ( $m/z$  weighted average  $\pm$  one standard deviation:  $367 \pm 57$ ) compared to the deep Pacific ( $504 \pm 84$ ; Fig. S5). This is in contrast to previous work showing an inverse relationship between molecular size and DOM diagenesis, age, and biological reactivity (Amon and Benner, 1996; Benner and Amon, 2015; Kaiser and Benner, 2009; Walker et al., 2014) as determined from size-fractionated extraction methods, but is similar to results from other SPE-DOM samples (Flerus et al., 2012; Hertkorn et al., 2013). We cannot directly determine the processes contributing to these differences in composition from these data, but possible explanations could include the production or accumulation of larger molecules as analyzed by this technique within

the DOM pool as it moves along the deep conveyor belt to the Pacific via thermohaline circulation or the selective removal of smaller compounds produced in the northeast Atlantic.

Compounds that have higher average normalized intensities in MEDEA samples also have a lower average O/C ratio compared to the NEqPIW SPE-DOM, showing a similar trend to what was observed between the subsurface and deep northeast Atlantic. This elevation in O/C in the North Pacific was also detected by Chen et al. (2014), and implies that similar processes might contribute to the increase in oxygen content of compounds in DOM from subsurface to deep in the northeast Atlantic water column and between the Atlantic and Pacific basins.

$I_{\text{deg}}$  for the NEqPIW reference was  $0.855 \pm 0.010$  (average  $\pm$  one standard deviation,  $n = 47$ ), higher than any sample in our MEDEA data set with its highest average  $I_{\text{deg}}$  of  $0.774 \pm 0.019$  from LDW (Table 2). This difference in degradation and by proxy relative age of the SPE-DOM pool corresponds well to the published radiocarbon ages of DOC from the North Pacific of  $\sim 6000$  years compared to  $\sim 4000$  years in the deep North Atlantic (Bauer et al., 1992; Druffel et al., 1992; Williams and Druffel, 1987), further supporting the utility of this index in estimating the relative age of marine DOM.

### 3.6. Molecular composition of NEADW SPE-DOM

This data set offered a unique opportunity to analyze the molecular composition of SPE-DOM within the core of NEADW along a transect of more than 5000 km from the site of deep water formation in the North Atlantic southward to  $24^\circ\text{N}$ . Using the mixing model described by Reinthaler et al. (2013), we calculated the contribution of four specific water types (LSW, ISOW, LDW, MSOW) to the sampled NEADW core, with the results shown in Table S2 and Fig. S6. The results of the model are similar to that of Reinthaler et al. (2013), with ISOW and LSW comprising most of the NEADW in the northern part of the transect (nearly 90% at  $60^\circ\text{N}$ ) and decreasing to a minimum of around 20% in the south. The changing contributions of ISOW and LSW to NEADW are generally

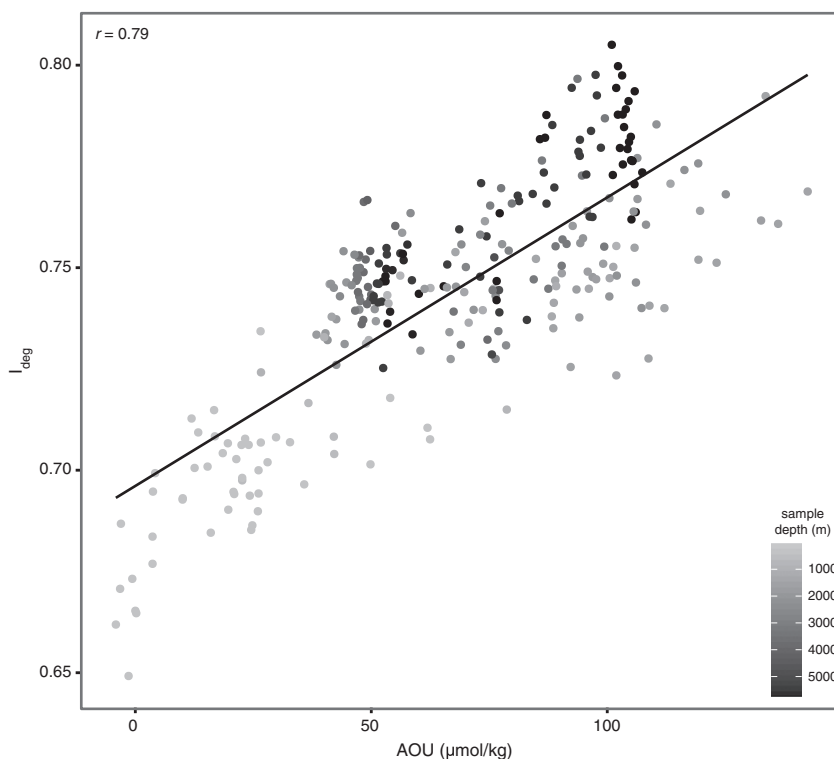


**Fig. 5.** Linear relationship between degradation index ( $I_{\text{deg}}$ ) (Flerus et al., 2012) of SPE-DOM samples calculated from FT-ICR-MS data and apparent oxygen utilization (AOU) for entire MEDEA data set. Gray scale indicates sample depth.  $r$  is Pearson product-moment correlation coefficient.

balanced by LDW, which increases southward along the transect from 8% to >70%. MSOW constituted less than 5% of NEADW throughout our study area, with its maximum contribution calculated from samples collected near 32°N.

We used these model results to test the conservation of SPE-DOM composition with mixing by calculating the expected molecular composition (peak masses and normalized intensities) for each sample in the NEADW using the average SPE-DOM molecular composition of identified end-members within the data set (Table S2). For the mixing model, average values from 4 to 6 samples were considered for each end-member. The generated synthetic data set for the conservative mixing case is therefore largely free of analytical variability. No true end-member for MSOW was sampled during our MEDEA cruises; however, because the maximum contribution of MSOW to the sampled NEADW core was determined to be less than 5% (Fig. S6b), we excluded MSOW from our calculated NEADW SPE-DOM composition.

Generally, this calculated SPE-DOM composition predicted the composition of NEADW SPE-DOM we measured in our samples very well, as shown by the linear relationship between the calculated and the actual Bray–Curtis dissimilarities for each sample within the NEADW core, relative to the southernmost sample collected at 24.67°N (Fig. 6; Pearson product–moment correlation coefficient  $r$  of 0.79;  $p < 0.001$ ). Fig. 6 shows that the actual Bray–Curtis dissimilarity for NEADW SPE-DOM samples increases with latitude compared to the southernmost sample, and these relatively small changes in SPE-DOM composition were accurately reflected in the calculated data set as well. Therefore, it appears that the molecular composition of SPE-DOM within the NEADW is conserved and primarily due to the mixing of water masses.

There are some small differences between the actual and calculated data, and the averages of these are plotted against  $m/z$  in Fig. S7. However these differences are not significantly correlated with the proportion of MSOW for each sample, and appear to be within our analytical variability (average Bray–Curtis dissimilarity between actual and calculated data  $\pm$  one standard deviation was  $5.6 \pm 2.1\%$ ). No correlations between these differences and specific masses or groups of molecules

could be established. Reinthaler et al. (2013) noted that localized microbial activity explained a large fraction of the microbial parameters measured in the NEADW core, but it appears that these same processes have little effect on the composition of the SPE-DOM pool relative to mixing.

We also determined  $I_{deg}$  for the calculated NEADW data set, and compared this to the measured  $I_{deg}$  to evaluate the impact of conservative mixing versus non-conservative processes on this parameter. Based on the linear relationship between actual and calculated  $I_{deg}$  ( $r^2 = 0.60$ ,  $p < 0.001$ ; Fig. S8), we conclude that the conservative mixing model predicts most of the  $I_{deg}$  variation measured in the NEADW samples. AOU is also a conservative parameter within the NEADW core ( $r^2 = 0.92$ ,  $p < 0.001$ ), so conservation of  $I_{deg}$  is not surprising given its close link to apparent water mass age.

### 3.7. Low variation in SPE-DOM molecular composition

The overall similarity of the molecular composition of SPE-DOM in the northeast Atlantic is surprising given the strong physical, chemical, and biological gradients that exist both vertically and laterally throughout this ocean basin. Pronounced changes with latitude and depth in the activity and composition of the microbial community have been reported for the North Atlantic (Agogué et al., 2011; Reinthaler et al., 2006). Albeit these pronounced vertical gradients in heterotrophic microbial activity, the molecular composition of the SPE-DOM pool is strikingly invariable with depth. However, this may be a consequence of the technique and timescales on which the molecular composition of DOM is evaluated here. Rapid removal of labile DOM within hours and the subsequent production of compounds through the degradation of labile DOM by heterotrophic microbes on these same timescales would preclude the dynamics of these portions of the pool being captured through single discrete samples. Thus, our data likely reflect the composition of marine DOM after these processes occur. In essence, we measure the “leftovers,” which may explain the disconnect between DOM composition and microbial water mass specificity. Our results indicate that the accumulation of less reactive compounds creates a large background

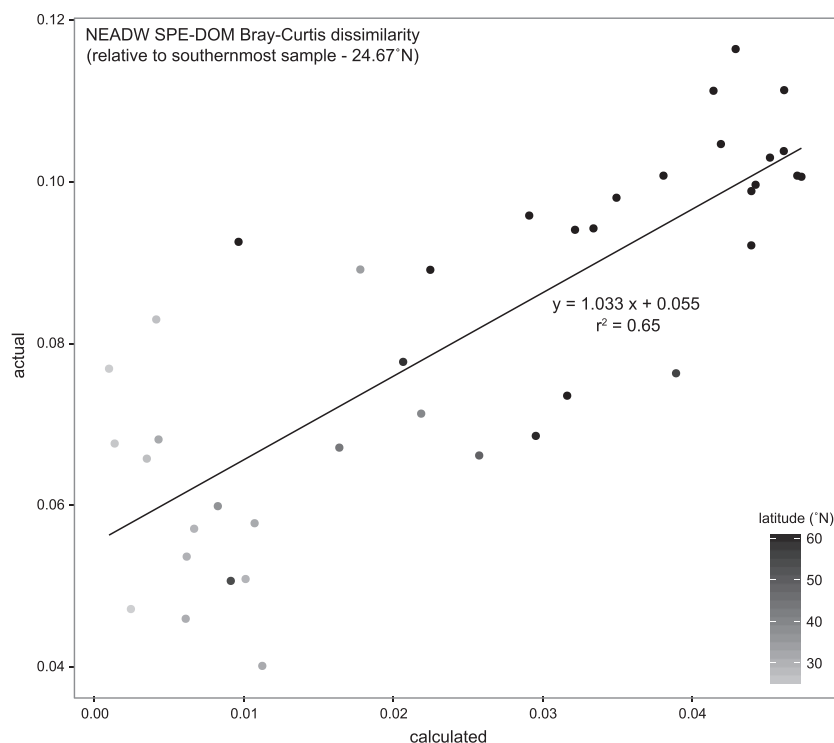


**Fig. 6.** Linear relationship between the Bray–Curtis dissimilarities, relative to the southernmost sample (24.67°N), for actual NEADW SPE-DOM compositions and those calculated assuming conservative mixing. Gray scale indicates latitude of sample collection.

signal that dominates the molecular composition of SPE-DOM in the deep ocean. In contrast, the more active and abundant members dominate the phylogenetic signature of the microbial community. Hence, while our SPE-DOM analysis using FT-ICR-MS largely covers the 'inert' part of the DOM, the microbial community analysis covers the active and dynamic part of the microbial community. Thus, the SPE-DOM spectrum we analyzed in this paper is characterized by a long molecular memory matching the long residence time of portions of the deep DOM pool (Follett et al., 2014). Alternatively, the chemical complexity of DOM results in individual molecules that are too dilute for consumption by the microbial community (Arrieta et al., 2015), thus the low concentrations of these compounds rather than their inherent reactivity lead to the overall background signal we observe in deep ocean SPE-DOM.

Our method of DOM isolation may also contribute to the observed low variability. SPE was selected as a relatively simple method for desalting and concentrating marine DOM but of course only captures a portion of the total pool. Extraction efficiencies for our SPE-DOM are not available, but this method typically yields > 60% of deep marine DOC (e.g., Green et al., 2014; Stubbins et al., 2012). Therefore, the fraction of DOM missing from our analyses may include more variable components of the DOM pool. However, comparison of our northeast Atlantic samples to the NEqPIW reference does reveal more pronounced differences between the molecular composition of the DOM pools isolated by SPE from the two ocean basins. Additionally, the differences we did observe between subsurface and deep northeast Atlantic SPE-DOM composition, as well as those between the North Atlantic and North Pacific, were similar to the variations identified in DOM isolated by the coupled reverse osmosis–electrodialysis method (Chen et al., 2014). This indicates that SPE is sufficient for capturing compounds that contribute to ocean-scale variability in the DOM pool.

#### 4. Conclusions

Although the various water masses of the North Atlantic exhibit characteristic physical, chemical, and biological properties, the molecular composition of SPE-DOM as assessed by FT-ICR-MS does not show this same specificity, and in fact is remarkably similar throughout the water column of the northeast Atlantic. However, small variations can be found between subsurface and deep waters, as well as among latitudinal provinces, and these are reflected through differences in the molecular weight and elemental composition of compounds within the SPE-DOM pool. Certain components of marine DOM, like the molecules used for calculating the degradation index ( $I_{deg}$ ), do show changes with depth and water mass age in the North Atlantic. The strong correlation between  $I_{deg}$  and AOU may be interpreted as a result of DOM aging in the deep sea (Flerus et al., 2012). However, remarkable similarities between actual and calculated molecular SPE-DOM compositions of the NEADW demonstrate that the molecular composition of SPE-DOM is primarily a conservative parameter constrained by mixing water masses. Thus, the apparent aging of DOM in the deep sea is likely the simple result of mixing of different DOM pools. In consequence, aging of DOM largely occurs at the sea surface and the source of deep water masses. The source signal is then largely preserved in the deep sea for extended periods of time. The apparent stability of the molecular signature of SPE-DOM is in sharp contrast to the variability of the microbial community in the deep ocean. More pronounced changes in SPE-DOM composition were observed when comparing the northeast Atlantic to the deep North Pacific, indicating that processes affecting the molecular composition of the DOM pool do occur on much larger spatial and temporal scales than captured during water mass formation and transport in the North Atlantic.

#### Acknowledgments

We would like to thank the captain and crew of the RV *Pelagia* for their support during the MEDEA cruises, Jan van Ooijen for the nutrient

analyses, and Santiago Gonzales for measuring dissolved oxygen. Ina Ulber and Jutta Niggemann were very helpful with the preparation and advice for SPE-DOM sampling. Many thanks to Katrin Klaproth for help with sample prep and analysis on the FT, as well as with initial data processing. Funding was provided by the European Research Council under the European Community's Seventh Framework Program (FP7/2007-2013)/ERC grant agreement No. 268595 (MEDEA project) and the Austrian Science Fund (FWF) project I486-B09 both to GJH.

#### Appendix A. Supplementary data

Supplementary data to this article can be found online at <http://dx.doi.org/10.1016/j.marchem.2015.06.001>.

#### References

- Agogué, H., Brink, M., Dinasquet, J., Herndl, G.J., 2008. Major gradients in putatively nitrifying and non-nitrifying Archaea in the deep North Atlantic. *Nature* 456, 788–791. <http://dx.doi.org/10.1038/nature07535>.
- Agogué, H., Lamy, D., Neal, P.R., Sogin, M.L., Herndl, G.J., 2011. Water mass-specificity of bacterial communities in the North Atlantic revealed by massively parallel sequencing. *Mol. Ecol.* 20, 258–274. <http://dx.doi.org/10.1111/j.1365-294X.2010.04932.x>.
- Aluwihare, L.I., Repeta, D.J., Chen, R.F., 1997. A major biopolymeric component to dissolved organic carbon in surface sea water. *Nature* 387, 166–169. <http://dx.doi.org/10.1038/387166a0>.
- Álvarez, M., Pérez, F.F., Bryden, H., Ríos, A.F., 2004. Physical and biogeochemical transports structure in the North Atlantic subpolar gyre. *J. Geophys. Res.* 109, C03027. <http://dx.doi.org/10.1029/2003JC002015>.
- Amon, R.M.W., Benner, R., 1996. Bacterial utilization of different size classes of dissolved organic matter. *Limnol. Oceanogr.* 41, 41–51.
- Anderson, M.J., Willis, T.J., 2003. Canonical analysis of principal coordinates: a useful method of constrained ordination for ecology. *Ecology* 84, 511–525.
- Arrieta, J.M., Mayol, E., Hansman, R.L., Herndl, G.J., Dittmar, T., Duarte, C.M., 2015. Dilution limits dissolved organic carbon utilization in the deep ocean. *Science* 348, 331–333. <http://dx.doi.org/10.1126/science.1258955>.
- Azam, F., Fenchel, T., Field, J.G., Gray, J.S., Meyer-Reil, L.A., Thingstad, F., 1983. The ecological role of water-column microbes in the sea. *Mar. Ecol. Prog. Ser.* 10, 257–263.
- Bauer, J.E., Williams, P.M., Druffel, E.R.M., 1992. C-14 activity of dissolved organic-carbon fractions in the North-Central Pacific and Sargasso Sea. *Nature* 357, 667–670. <http://dx.doi.org/10.1038/357667a0>.
- Benner, R., 2002. Chapter 3 – chemical composition and reactivity. In: Hansell, Dennis A., Carlson, Craig A. (Eds.), *Biogeochemistry of Marine Dissolved Organic Matter*. Academic Press, San Diego, pp. 59–90.
- Benner, R., Amon, R.M.W., 2015. The size-reactivity continuum of major bioelements in the ocean. *Ann. Rev. Mar. Sci.* 7. <http://dx.doi.org/10.1146/annurev-marine-010213-135126> (null).
- Benner, R., Pakulski, J.D., McCarthy, M., Hedges, J.I., Hatcher, P.G., 1992. Bulk chemical characteristics of dissolved organic matter in the ocean. *Science* 255, 1561–1564. <http://dx.doi.org/10.1126/science.255.5051.1561>.
- Carlson, C.A., 2002. Chapter 4 – production and removal processes. In: Hansell, Dennis A., Carlson, Craig A. (Eds.), *Biogeochemistry of Marine Dissolved Organic Matter*. Academic Press, San Diego, pp. 91–151.
- Carlson, C.A., Hansell, D.A., Nelson, N.B., Siegel, D.A., Smethie, W.M., Khatiwala, S., Meyers, M.M., Halewood, E., 2010. Dissolved organic carbon export and subsequent remineralization in the mesopelagic and bathypelagic realms of the North Atlantic basin. *Deep-Sea Res. II Top. Stud. Oceanogr.* 57, 1433–1445. <http://dx.doi.org/10.1016/j.dsr2.2010.02.013>.
- Chen, H., Stubbins, A., Perdue, E.M., Green, N.W., Helms, J.R., Mopper, K., Hatcher, P.G., 2014. Ultrahigh resolution mass spectrometric differentiation of dissolved organic matter isolated by coupled reverse osmosis-electrodialysis from various major oceanic water masses. *Mar. Chem.* 164, 48–59. <http://dx.doi.org/10.1016/j.marchem.2014.06.002>.
- Dittmar, T., Paeng, J., 2009. A heat-induced molecular signature in marine dissolved organic matter. *Nat. Geosci.* 2, 175–179. <http://dx.doi.org/10.1038/ngeo440>.
- Dittmar, T., Koch, B., Hertkorn, N., Kattner, G., 2008. A simple and efficient method for the solid-phase extraction of dissolved organic matter (SPE-DOM) from seawater. *Limnol. Oceanogr. Methods* 6, 230–235. <http://dx.doi.org/10.4319/lom.2008.6.230>.
- Druffel, E.R.M., Williams, P.M., Bauer, J.E., Ertel, J.R., 1992. Cycling of dissolved and particulate organic matter in the open ocean. *J. Geophys. Res. Oceans* 97, 15639–15659. <http://dx.doi.org/10.1029/92JC01511>.
- Flerus, R., Lechtenfeld, O.J., Koch, B.P., McCallister, S.L., Schmitt-Kopplin, P., Benner, R., Kaiser, K., Kattner, G., 2012. A molecular perspective on the ageing of marine dissolved organic matter. *Biogeosciences* 9, 1935–1955. <http://dx.doi.org/10.5194/bg-9-1935-2012>.
- Follett, C.L., Repeta, D.J., Rothman, D.H., Xu, L., Santinelli, C., 2014. Hidden cycle of dissolved organic carbon in the deep ocean. *PNAS* 111, 16706–16711. <http://dx.doi.org/10.1073/pnas.1407445111>.
- Gordon, L.L., Jennings Jr., J.C., Ross, A.A., Krest, J.M., 1993. A suggested protocol for continuous flow automated analysis of seawater nutrients (phosphate, nitrate, nitrite and silicic acid) in the WOCE Hydrographic Program and the Joint Global Ocean Fluxes Study. *OCE Operations Manual, Part 3* pp. 1–55.

- Green, N.W., Perdue, E.M., Aiken, G.R., Butler, K.D., Chen, H., Dittmar, T., Niggemann, J., Stubbins, A., 2014. An intercomparison of three methods for the large-scale isolation of oceanic dissolved organic matter. *Mar. Chem.* 161, 14–19. <http://dx.doi.org/10.1016/j.marchem.2014.01.012>.
- Hansell, D.A., 2013. Recalcitrant dissolved organic carbon fractions. *Ann. Rev. Mar. Sci.* 5, 421–445. <http://dx.doi.org/10.1146/annurev-marine-120710-100757>.
- Hansell, D.A., Carlson, C.A., 2001. Biogeochemistry of total organic carbon and nitrogen in the Sargasso Sea: control by convective overturn. *Deep-Sea Res. II Top. Stud. Oceanogr.* 48, 1649–1667. [http://dx.doi.org/10.1016/S0967-0645\(00\)00153-3](http://dx.doi.org/10.1016/S0967-0645(00)00153-3).
- Hansell, D., Carlson, C., Repeta, D., Schlitzer, R., 2009. Dissolved organic matter in the ocean: a controversy stimulates new insights. *Oceanography* 22, 202–211. <http://dx.doi.org/10.5670/oceanog.2009.109>.
- Hansell, D.A., Carlson, C.A., Schlitzer, R., 2012. Net removal of major marine dissolved organic carbon fractions in the subsurface ocean. *Glob. Biogeochem. Cycles* 26, GB1016. <http://dx.doi.org/10.1029/2011GB004069>.
- Hedges, J.L., 1992. Global biogeochemical cycles: progress and problems. *Mar. Chem.* 39, 67–93.
- Hertkorn, N., Benner, R., Frommberger, M., Schmitt-Kopplin, P., Witt, M., Kaiser, K., Ketrup, A., Hedges, J.L., 2006. Characterization of a major refractory component of marine dissolved organic matter. *Geochim. Cosmochim. Acta* 70, 2990–3010. <http://dx.doi.org/10.1016/j.gca.2006.03.021>.
- Hertkorn, N., Harir, M., Koch, B.P., Michalke, B., Schmitt-Kopplin, P., 2013. High-field NMR spectroscopy and FTICR mass spectrometry: powerful discovery tools for the molecular level characterization of marine dissolved organic matter. *Biogeosciences* 10, 1583–1624. <http://dx.doi.org/10.5194/bg-10-1583-2013>.
- Kaiser, K., Benner, R., 2009. Biochemical composition and size distribution of organic matter at the Pacific and Atlantic time-series stations. *Mar. Chem.* 113, 63–77. <http://dx.doi.org/10.1016/j.marchem.2008.12.004>.
- Kirchman, D.L., Suzuki, Y., Garside, C., Ducklow, H.W., 1991. High turnover rates of dissolved organic carbon during a spring phytoplankton bloom. *Nature* 352, 612–614. <http://dx.doi.org/10.1038/352612a0>.
- Koch, B.P., Dittmar, T., 2006. From mass to structure: an aromaticity index for high-resolution mass data of natural organic matter. *Rapid Commun. Mass Spectrom.* 20, 926–932. <http://dx.doi.org/10.1002/rcm.2386>.
- Koch, B.P., Witt, M., Engbrodt, R., Dittmar, T., Kattner, G., 2005. Molecular formulae of marine and terrigenous dissolved organic matter detected by electrospray ionization Fourier transform ion cyclotron resonance mass spectrometry. *Geochim. Cosmochim. Acta* 69, 3299–3308. <http://dx.doi.org/10.1016/j.gca.2005.02.027>.
- Koch, B.P., Dittmar, T., Witt, M., Kattner, G., 2007. Fundamentals of molecular formula assignment to ultrahigh resolution mass data of natural organic matter. *Anal. Chem.* 79, 1758–1763. <http://dx.doi.org/10.1021/ac061949s>.
- Kujawinski, E.B., Longnecker, K., Blough, N.V., Vecchio, R.D., Finlay, L., Kitner, J.B., Giovannoni, S.J., 2009. Identification of possible source markers in marine dissolved organic matter using ultrahigh resolution mass spectrometry. *Geochim. Cosmochim. Acta* 73, 4384–4399. <http://dx.doi.org/10.1016/j.gca.2009.04.033>.
- McCarthy, M.D., Hedges, J.L., Benner, R., 1998. Major bacterial contribution to marine dissolved organic nitrogen. *Science* 281, 231–234. <http://dx.doi.org/10.1126/science.281.5374.231>.
- Medeiros, P.M., Seidel, M., Powers, L.C., Dittmar, T., Hansell, D.A., Miller, W.L., 2015. Dissolved organic matter composition and photochemical transformations in the northern North Pacific Ocean. *Geophys. Res. Lett.* 42. <http://dx.doi.org/10.1002/2014GL026663> (2014GL026663).
- Oksanen, J., Blanchet, F.G., Kindt, R., Legendre, P., Minchin, P.R., O'Hara, R.B., Simpson, G.L., Solymos, P., Stevens, M.H.H., Wagner, H., 2013. *Vegan: Community Ecology Package*.
- Osterholz, H., Dittmar, T., Niggemann, J., 2014. Molecular evidence for rapid dissolved organic matter turnover in Arctic fjords. *Mar. Chem.* 160, 1–10. <http://dx.doi.org/10.1016/j.marchem.2014.01.002>.
- Pakulski, J.D., Benner, R., 1994. Abundance and distribution of carbohydrates in the ocean. *Limnol. Oceanogr.* 39, 930–940.
- Pan, X., Achterberg, E.P., Sanders, R., Poulton, A.J., Oliver, K.I.C., Robinson, C., 2014. Dissolved organic carbon and apparent oxygen utilization in the Atlantic Ocean. *Deep-Sea Res. I Oceanogr. Res. Pap.* 85, 80–87. <http://dx.doi.org/10.1016/j.dsr.2013.12.003>.
- Reinthal, T., van Aken, H., Veth, C., Aristegui, J., Robinson, C., Williams, P.J. le B., Lebaron, P., Herndl, G.J., 2006. Prokaryotic respiration and production in the meso- and bathypelagic realm of the eastern and western North Atlantic basin. *Limnol. Oceanogr.* 51, 1262–1273. <http://dx.doi.org/10.4319/lo.2006.51.3.1262>.
- Reinthal, T., Álvarez Salgado, X.A., Álvarez, M., van Aken, H.M., Herndl, G.J., 2013. Impact of water mass mixing on the biogeochemistry and microbiology of the Northeast Atlantic Deep Water. *Glob. Biogeochem. Cycles* 27, 1151–1162. <http://dx.doi.org/10.1002/2013GB004634>.
- Riedel, T., Dittmar, T., 2014. A method detection limit for the analysis of natural organic matter via Fourier Transform Ion Cyclotron Resonance Mass Spectrometry. *Anal. Chem.* 86, 8376–8382. <http://dx.doi.org/10.1021/ac501946m>.
- Schlitzer, R., 2013. *Ocean Data View*.
- Sintes, E., Bergauer, K., De Corte, D., Yokokawa, T., Herndl, G.J., 2013. Archaeal *amoA* gene diversity points to distinct biogeography of ammonia-oxidizing *Crenarchaeota* in the ocean: biogeography of archaeal ammonia oxidizers. *Environ. Microbiol.* 15, 1647–1658. <http://dx.doi.org/10.1111/j.1462-2920.2012.02801.x>.
- Stubbins, A., Niggemann, J., Dittmar, T., 2012. Photo-lability of deep ocean dissolved black carbon. *Biogeosciences* 9, 1661–1670. <http://dx.doi.org/10.5194/bg-9-1661-2012>.
- Team, R.C., 2014. *R: A Language and Environment for Statistical Computing*. R Foundation for Statistical Computing, Vienna, Austria.
- Van Aken, H.M., 2000a. The hydrography of the mid-latitude Northeast Atlantic Ocean: II: the intermediate water masses. *Deep-Sea Res. I Oceanogr. Res. Pap.* 47, 789–824. [http://dx.doi.org/10.1016/S0967-0637\(99\)00112-0](http://dx.doi.org/10.1016/S0967-0637(99)00112-0).
- Van Aken, H.M., 2000b. The hydrography of the mid-latitude northeast Atlantic Ocean: I: the deep water masses. *Deep-Sea Res. I Oceanogr. Res. Pap.* 47, 757–788. [http://dx.doi.org/10.1016/S0967-0637\(99\)00092-8](http://dx.doi.org/10.1016/S0967-0637(99)00092-8).
- Varela, M.M., van Aken, H.M., Herndl, G.J., 2008a. Abundance and activity of Chloroflexi-type SAR202 bacterioplankton in the meso- and bathypelagic waters of the (sub)-tropical Atlantic. *Environ. Microbiol.* 10, 1903–1911. <http://dx.doi.org/10.1111/j.1462-2920.2008.01627.x>.
- Varela, M.M., Van Aken, H.M., Sintes, E., Herndl, G.J., 2008b. Latitudinal trends of Crenarchaeota and bacteria in the meso- and bathypelagic water masses of the Eastern North Atlantic. *Environ. Microbiol.* 10, 110–124. <http://dx.doi.org/10.1111/j.1462-2920.2007.01437.x>.
- Walker, B.D., Guilderson, T.P., Okimura, K.M., Peacock, M.B., McCarthy, M.D., 2014. Radiocarbon signatures and size–age–composition relationships of major organic matter pools within a unique California upwelling system. *Geochim. Cosmochim. Acta* 126, 1–17. <http://dx.doi.org/10.1016/j.gca.2013.10.039>.
- Williams, P.M., Druffel, E.R.M., 1987. Radiocarbon in dissolved organic matter in the central North Pacific Ocean. *Nature* 330, 246–248. <http://dx.doi.org/10.1038/330246a0>.